

# Estimating regional ground-level PM<sub>2.5</sub> directly from satellite top-of-atmosphere reflectance using deep learning

Huanfeng Shen <sup>a,b,c,\*</sup>, Tongwen Li <sup>a</sup>, Qiangqiang Yuan <sup>d,b</sup>, Liangpei Zhang <sup>e,b</sup>

<sup>a</sup> School of Resource and Environmental Sciences, Wuhan University, Wuhan, China.

<sup>b</sup> The Collaborative Innovation Center for Geospatial Technology, Wuhan, China.

<sup>c</sup> The Key Laboratory of Geographic Information System, Ministry of Education, Wuhan University, Wuhan, China.

<sup>d</sup> School of Geodesy and Geomatics, Wuhan University, Wuhan, China.

<sup>e</sup> The State Key Laboratory of Information Engineering in Surveying, Mapping and Remote Sensing, Wuhan University, Wuhan, China.

\* Corresponding author: Huanfeng Shen (shenhf@whu.edu.cn)

## Highlights:

- We estimate ground PM<sub>2.5</sub> from satellite TOA reflectance rather than satellite AOD.
- The Ref-PM modeling achieves an outstanding performance for estimating ground PM<sub>2.5</sub>.
- Daily fine-scale distributions of PM<sub>2.5</sub> are mapped in Wuhan Urban Agglomeration.

## ABSTRACT

Almost all remote sensing atmospheric PM<sub>2.5</sub> estimation methods need satellite aerosol optical depth (AOD) products, which are often retrieved from top-of-atmosphere (TOA) reflectance via an atmospheric radiative transfer model. Then, is it possible to estimate ground-level PM<sub>2.5</sub> directly from satellite TOA reflectance without a physical model? In this study, this challenging work are achieved based on a machine learning model. Specifically, we establish the relationship between PM<sub>2.5</sub>, satellite TOA reflectance, observation angles, and meteorological factors in a deep learning architecture (denoted as Ref-PM modeling). Taking the Wuhan Urban Agglomeration (WUA) as a case study, the results demonstrate that compared with the AOD-PM modeling, the Ref-PM modeling obtains a competitive performance, with out-of-sample cross-validated R<sup>2</sup> and RMSE values of 0.87 and 9.89  $\mu\text{g} / \text{m}^3$  respectively. Also, the TOA-reflectance-derived PM<sub>2.5</sub> have a finer resolution and larger spatial coverage than the AOD-derived PM<sub>2.5</sub>. This work updates the traditional cognition of remote sensing PM<sub>2.5</sub> estimation and has the potential to promote the application in atmospheric environmental monitoring.

**Keywords:** PM<sub>2.5</sub>, satellite remote sensing, TOA reflectance, deep learning

## 1. Introduction

Fine particular matter (PM<sub>2.5</sub>, airborne particles less than 2.5  $\mu\text{m}$  in the aerodynamic diameter) has been reported to be associated with many adverse health effects including cardiovascular and respiratory morbidity and mortality (Habre et al., 2014; Madrigano et al., 2013). Previous studies have indicated that the severe PM<sub>2.5</sub> pollution resulted in more than 3 million premature deaths around the world in the year of 2010 (Lim et al., 2012). It is thus an urgent need to acquire accurate spatiotemporal distributions of ground-level PM<sub>2.5</sub> concentration for the environmental health concerns.

The satellite-derived aerosol optical depth (AOD) products have been extensively employed to expand PM<sub>2.5</sub> estimation beyond that only provided by ground monitoring stations (Hoff and Christopher 2009; Li et al., 2016; van Donkelaar et al., 2016). The AOD products used include those retrieved from the Moderate Resolution Imaging Spectroradiometer (MODIS) (Fang et al., 2016), the Multiangle Imaging SpectroRadiometer (MISR) (You et al., 2015), the Geostationary Operational Environmental Satellite Aerosol/Smoke Product (GASP) (Paciorek et al., 2008), the Visible Infrared Imaging Radiometer Suite (VIIRS) (Wu et al., 2016), etc. In addition, many models were developed to establish the relationship between AOD and PM<sub>2.5</sub> (denoted as AOD-PM modeling), such as multiple linear regression (MLR) (Gupta and Christopher 2009b), geographically weighted regression (GWR) (Hu et al., 2013), linear mixed effects (LME) model (Lee et al., 2011), neural networks (NN) (Gupta and Christopher 2009a; Li et al., 2017b), and so on. Based on these models, the satellite-derived AOD products have played an important role in the estimation of ground-level PM<sub>2.5</sub>.

The AOD products are often retrieved from satellite top-of-atmosphere (TOA) reflectance through an atmospheric radiative transfer model (e.g., 6S, MODTRAN) (Hsu et al., 2004; Kaufman et al., 1997; Levy et al., 2007). Hence, the procedure of previous satellite-based  $PM_{2.5}$  estimation is usually to retrieve AOD from satellite TOA reflectance firstly, and subsequently estimate ground-level  $PM_{2.5}$  from satellite-derived AOD. A challenging proposition is that whether it is possible to avoid the intermediate process of AOD retrieval, and to estimate ground-level  $PM_{2.5}$  directly from satellite TOA reflectance (denoted as Ref-PM modeling). Actually, previous studies have provided some potentials for the Ref-PM modeling. On the one hand, some researchers (Radosavljevic et al., 2007; Ristovski et al., 2012) adopted neural networks to learn a functional relationship between MODIS observations and ground-observed AOD, and the neural-network-based AOD retrievals achieved satisfactory results compared with the physically retrieved AOD in their experiments. On the other hand, many aforementioned models have been employed to establish the AOD- $PM_{2.5}$  relationship. Given that the physical retrieval of AOD from TOA reflectance can be simulated using statistical approaches, as well as the AOD- $PM_{2.5}$  relationship, it appears possible to directly model the statistical relationship between TOA reflectance and ground-level  $PM_{2.5}$ .

Anyhow, it would be very complicated to estimate ground-level  $PM_{2.5}$  from satellite TOA reflectance in one step. The retrieval of AOD from satellite TOA reflectance is a nonlinear physical problem; the satellite-derived AOD in conjunction with auxiliary factors (e.g., meteorological parameters) are also usually nonlinearly correlated with  $PM_{2.5}$ . Hence, the estimation of ground-level  $PM_{2.5}$  directly from TOA reflectance is of high complexity, and the

conventional models may encounter some challenges. Deep learning, which is the further development of neural network, has been used for time-series predictions (Ong et al., 2015) and satellite AOD-based estimation (Li et al., 2017a) of ground-level  $PM_{2.5}$ . The deep learning models have shown the capacity to effectively predict/estimate ground-level  $PM_{2.5}$ , which can be attributed to its capacity of fitting nonlinear and complicated relationship (Hinton et al., 2006). Thus, deep learning may be a good tool for the satellite TOA reflectance-based estimation of ground-level  $PM_{2.5}$ .

The objective of this study is to develop a deep learning-based modeling for the estimation of ground-level  $PM_{2.5}$  using satellite TOA reflectance rather than AOD products. To be specific, one of the most typical deep learning models (i.e., deep belief network) will be employed to establish the relationship between ground-level  $PM_{2.5}$ , satellite TOA reflectance, observation angles, and meteorological factors. Through the Ref-PM modeling, we can not only simplify the procedure of satellite-based  $PM_{2.5}$  estimation, but also avert the accumulative error of AOD retrieval, which has been reported in previous studies (Munchak et al., 2013). The proposed Ref-PM modeling will be validated with the data from Wuhan Urban Agglomeration (Fig. 1) in the whole year of 2016.

## **2. Study region and data**

### *2.1. Study region*

The study region is Wuhan Urban Agglomeration (WUA), which is presented in Fig. 1. The study period is a total year of 2016. WUA is located in Hubei province, central China (as shown in Fig. 1 (a) and (b)). To make full use of  $PM_{2.5}$  station measurements, the monitoring stations in the range with latitude of  $28.4^{\circ} \sim 32.3^{\circ} \text{N}$  and longitude of  $112.0^{\circ} \sim 116.7^{\circ} \text{E}$  are all

adopted in our analysis. WUA is a city group with the center of Wuhan, covering the vicinal 8 cities (Huangshi, Ezhou, Huanggang, Xiaogan, Xianning, Xiantao, Qianjiang, and Tianmen). It has the total population of greater than 30 million, which account for more than a half of the total population of Hubei province. With over 60% of Gross Domestic Product (GDP) of Hubei province, WUA is one of the largest urban groups in central China. In 2007, it is authorized as one of the reforming pilot areas for national resource-saving and environment-friendly society by the Chinese government.

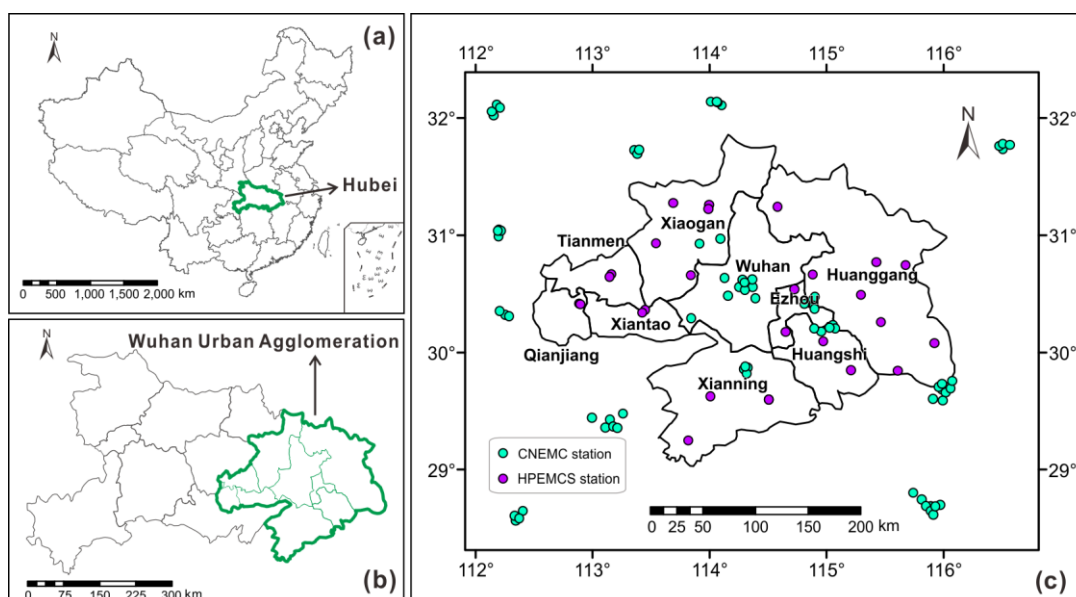


**Fig. 1.** Study region and the spatial distribution of PM<sub>2.5</sub> stations. (a) The location of Hubei province in China. (b) The boundary of Wuhan Urban Agglomeration in Hubei province. (c) The Wuhan Urban Agglomeration and the distribution of PM<sub>2.5</sub> monitoring stations.

Due to the dense urbanization and industrial activities, WUA has been suffering serious air pollution. Wuhan is especially populated with fine-mode particles (Wang et al., 2015), and the mean atmospheric PM<sub>2.5</sub> mass concentration was about  $160 \pm 50 \mu\text{g} / \text{m}^3$  (Wang et al., 2014). Moreover, with the rapid economic development, the other cities in WUA (e.g., Ezhou and Huangshi) also have a high level of PM<sub>2.5</sub> concentration. It is thus very urgent and necessary to obtain the spatiotemporal distributions of PM<sub>2.5</sub> in this area.

## 2.2. Ground-level $PM_{2.5}$ measurements

Hourly  $PM_{2.5}$  concentration data within the study region in 2016 were obtained from the China National Environmental Monitoring Center (CNEMC) website (<http://www.cnemc.cn>) and the Hubei Provincial Environmental Monitoring Center Station (HPEMCS) website (<http://www.hbemc.com.cn/>). In this study, 77 CNEMC stations and 27 HPEMCS stations (104 stations in total) are included. The distribution of  $PM_{2.5}$  monitoring stations is shown in Fig. 1 (c). It can be found that the CNEMC stations are unevenly distributed, while the HPEMCS stations make a good compensation. According to the Chinese National Ambient Air Quality Standard (CNAAQs, GB3905-2012), the ground  $PM_{2.5}$  concentrations are measured by the tapered element oscillating microbalance method (TEOM) or with beta attenuation monitors (BAMs or beta-gauge), with an uncertainty of 0.75% for the hourly record (Engel-Cox et al., 2013). We averaged hourly  $PM_{2.5}$  to daily mean  $PM_{2.5}$  data for the satellite-based estimation of  $PM_{2.5}$ . For each monitoring station, the dates with less than 18 hourly observations were excluded in our analysis.

## 2.3. Satellite observations

The Aqua Moderate Resolution Imaging Spectroradiometer (MODIS) Level 1B calibrated radiances (MYD02) product was downloaded from the Level 1 and Atmosphere Archive and Distribution System (LAADS) website (<https://ladsweb.modaps.eosdis.nasa.gov>). They have a spatial resolution of 1 km at nadir. The top-of-atmosphere reflectance on bands 1, 3 and 7 (R1, R3 and R7), and observation angles (i.e., sensor azimuth, sensor zenith, solar azimuth and solar zenith), were exploited for the retrieval of AOD via dark-target-based algorithms (Kaufman et al., 1997). Despite of the avoidance of AOD retrieval, these parameters were still

extracted from this product to estimate ground-level  $PM_{2.5}$ . To eliminate the cloud contamination, the MODIS cloud mask product (MYD35\_L2) was adopted. They are available at a resolution of 1 km every day. The cloud mask products have four confidence levels, i.e., “cloudy”, “uncertain clear”, “probably clear”, and “confident clear” (Ackerman et al., 1998). In this study, we only adopted the data with the highest confidence level (“confident clear”).

Furthermore, the MODIS normalized difference vegetation index (NDVI) product (Level 3, MYD13) with a resolution of 1 km every 16 days, were also downloaded from the LAADS website. The MODIS NDVI was incorporated into the  $PM_{2.5}$  estimation model to reflect the land cover type. For a comparison purpose, the MODIS aerosol optical depth (AOD) products of Collections 6 were utilized to establish the AOD-PM modeling. They have a spatial resolution of 3 km. The 3-km AOD products were retrieved using the dark-target-based algorithm (Munchak et al., 2013).

#### *2.4. Meteorological data*

The level of  $PM_{2.5}$  concentration is associated with meteorological parameters (Yang et al., 2017), the Goddard Earth Observing System Data Assimilation System GEOS-5 Forward Processing (GEOS 5-FP) (Lucchesi 2013) meteorological data were incorporated in this study. GEOS 5-FP exploits an analysis developed jointly with NOAA’s National Centers for Environmental Prediction (NCEP), which allows the Global Modeling and Assimilation Office (GMAO) to take advantage of the developments at NCEP and the Joint Center for Satellite Data Assimilation (JCSDA). The reanalysis meteorological data have a spatial resolution of  $0.25^\circ$  latitude  $\times$   $0.3125^\circ$  longitude. We extracted relative humidity (RH, %), air

temperature at a 2 m height (TMP, K), wind speed at 10 m above ground (WS, m/s), surface pressure (PS, kPa), and planetary boundary layer height (PBL, m) between 1 p.m. and 2 p.m. local time (the Aqua satellite overpass time corresponds to 1:30 p.m. local time). More details can be found at its official website (<https://gmao.gsfc.nasa.gov/forecasts/>).

### *2.5. Data pre-processing and matching*

Firstly, we created a 0.01-degree grid and a 0.03-degree grid for the Ref-PM modeling and the AOD-PM modeling, respectively. The data matching, model establishment, and spatial mapping are based on the established grids. For each grid, ground-level PM<sub>2.5</sub> measurements from multiple stations are averaged. Meanwhile, we resampled the meteorological data to match with satellite observations. All these data were re-projected to the same coordinate system. Finally, we extracted satellite observations, meteorological parameters on the locations where the PM<sub>2.5</sub> measurements are available.

## **3. Deep learning-based Ref-PM modeling for the estimation of PM<sub>2.5</sub>**

In the process of AOD retrieval, the satellite TOA reflectance bands and observation angles are utilized as the primary input. Also, an atmospheric radiative transfer model is exploited to simulate the physical relationship between reflectance, aerosol mode, and observation geometry. Though the Ref-PM modeling is aimed to avoid the complicated process of AOD retrieval, and to estimate ground-level PM<sub>2.5</sub> directly from satellite TOA reflectance, the original input (i.e., TOA reflectance and observation angles) are still adopted for the estimation of ground-level PM<sub>2.5</sub>.

Generally, the structure of the Ref-PM modeling is depicted as Eq. (1). The dependent variable is PM<sub>2.5</sub> concentration; and the input predictors are satellite TOA reflectance,

observation angles, meteorological parameters, and satellite NDVI. Additionally, we incorporated the geographical correlation of  $PM_{2.5}$  into the Ref-PM modeling. Because the nearby  $PM_{2.5}$  from neighboring  $s$  grids and the  $PM_{2.5}$  observations from prior  $t$  days for the same grid are informative for estimating  $PM_{2.5}$ . Here,  $s, t$  are set as 5 and 3 respectively.

$$PM_{2.5} = f(R1, R3, R7, angles, RH, WS, TMP, PBL, PS, NDVI, S-PM_{2.5}, T-PM_{2.5}, DIS) \quad (1)$$

where  $S-PM_{2.5}, T-PM_{2.5}, DIS$  denotes the geographical correlation of  $PM_{2.5}$ , and their calculations can refer to our previous study (Li et al., 2017a).  $R7$ , which is slightly influenced by atmosphere, reflects the surface reflectance.  $R1$  and  $R3$  can reflect the surface-atmosphere coupled reflectance on red and blue channels, and the surface reflectance can be separated using an empirical relationship (e.g., dark target algorithm (Kaufman et al., 1997)). Hence, the impact of atmosphere on satellite TOA reflectance signals can be separated from these input variables, and this is the basic principle and key point for remote sensing of  $PM_{2.5}$ .

The relationship between  $PM_{2.5}$ , satellite TOA reflectance, observation angles and meteorological factors is very complicated. Thus, deep learning, which has great potential for fitting the nonlinear and complex relationship, was employed to represent this relationship. To be specific, one of the most typical deep learning models (i.e., deep belief network, DBN) (Hinton et al., 2006) was adopted. Fig. 2 presents the structure of a DBN model containing two hidden layers. As illustrated in the figure, the basic unit is a restricted Boltzmann machine (RBM). An RBM contains a visible layer and a hidden layer, where the hidden layer of the prior RBM is the visible layer of the next RBM. The DBN consists of multiple RBMs and a back-propagation (BP) layer. This BP layer can be utilized for classification or prediction, and it is here used for the prediction of ground-level  $PM_{2.5}$ . In this study, two RBM layers with 15

neurons in each RBM layer are adopted. The details of the DBN model can refer to Li et al., (2017a). The procedure of this model for the Ref-PM modeling is divided to three steps, which is shown in Fig.3.

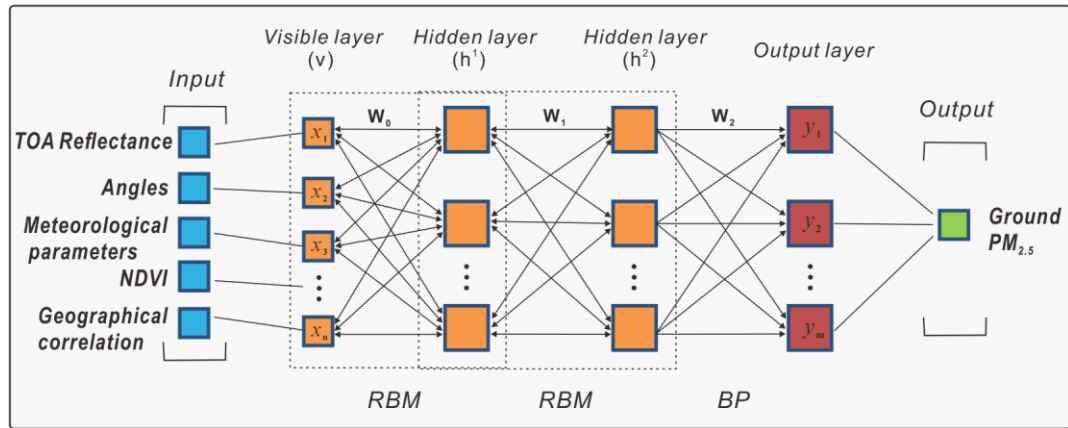


**Fig. 2.** The structure of DBN model for the Ref-PM modeling.

**Step 1:** The satellite TOA reflectance, observation angles, meteorological parameters, NDVI, and geographical correlation of  $PM_{2.5}$  are input into the DBN model. This model is pre-trained without supervision to initialize itself. That is, the station  $PM_{2.5}$  measurements are not used in this step, the initial model coefficients are trained from input data.

**Step 2:** The estimated  $PM_{2.5}$  can be obtained from the DBN model. Subsequently, we calculate mean square error (MSE) between estimated  $PM_{2.5}$  and ground observed  $PM_{2.5}$ . The error is sent back to fine-tune the model coefficients using the back-propagation (BP) algorithm (Rumelhart et al., 1986). This process will be repeated until the model achieves a satisfactory performance. Through this step, the DBN model can effectively establish the relationship between  $PM_{2.5}$  and satellite reflectance.

**Step 3:** The model will be validated and exploited to predict the  $PM_{2.5}$  values for those locations with no ground monitoring stations. Thus, the distribution of  $PM_{2.5}$  concentrations can be acquired.

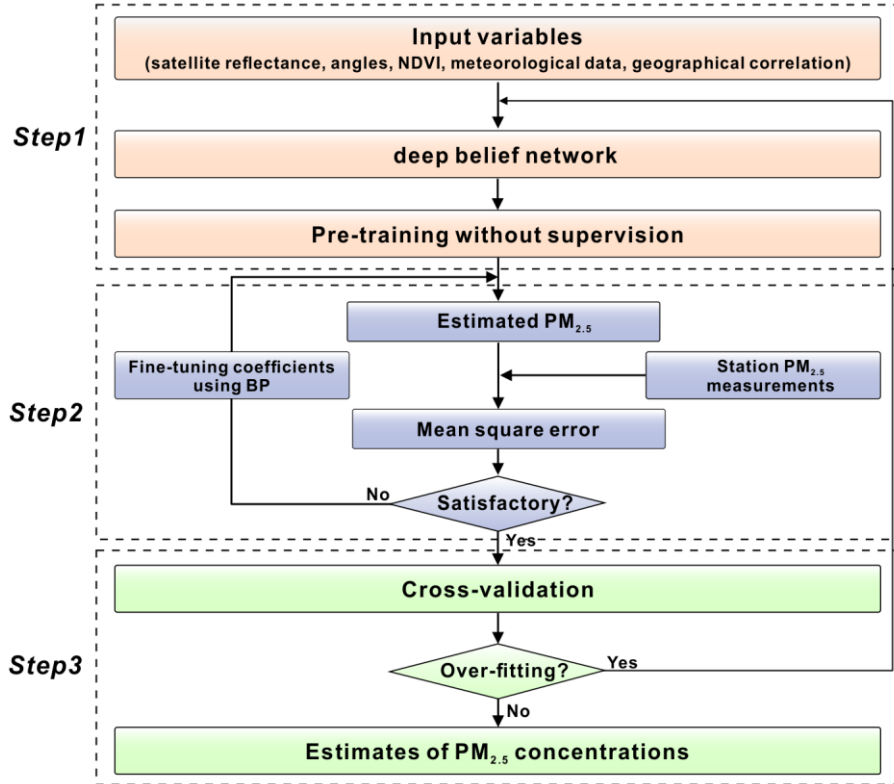


**Fig. 3.** Flowchart describing the process of DBN model for the Ref-PM modeling.

A 10-fold cross-validation (CV) technique (Rodriguez et al., 2010) was adopted to test the potential of model overfitting and predictive power. Previous studies usually used sample-based CV (Li et al., 2017b; Ma et al., 2014) or site-based CV (Lee et al., 2011; Xie et al., 2015) to evaluate the model performance. In this study, both sample-based CV and site-based CV were chosen for the model validation. For sample-based CV, all samples in the model dataset were randomly and equally divided into ten subsets. One subset was used as validation samples and the rest subsets were used to fit the model for each round of validation. For site-based CV, we divided the monitoring stations into ten subsets randomly and equally. One subset was used for validation and the remaining stations for model fitting in each round. We adopted the statistical indicators of the coefficient of determination ( $R^2$ ), the root-mean-square error (RMSE,  $\mu g / m^3$ ), the mean prediction error (MPE,  $\mu g / m^3$ ), and the

relative prediction error (RPE, defined as RMSE divided by the mean ground-level  $PM_{2.5}$ ) to give a quantitative evaluation of the model performance.

## 4. Results and discussion

### 4.1. Descriptive statistics

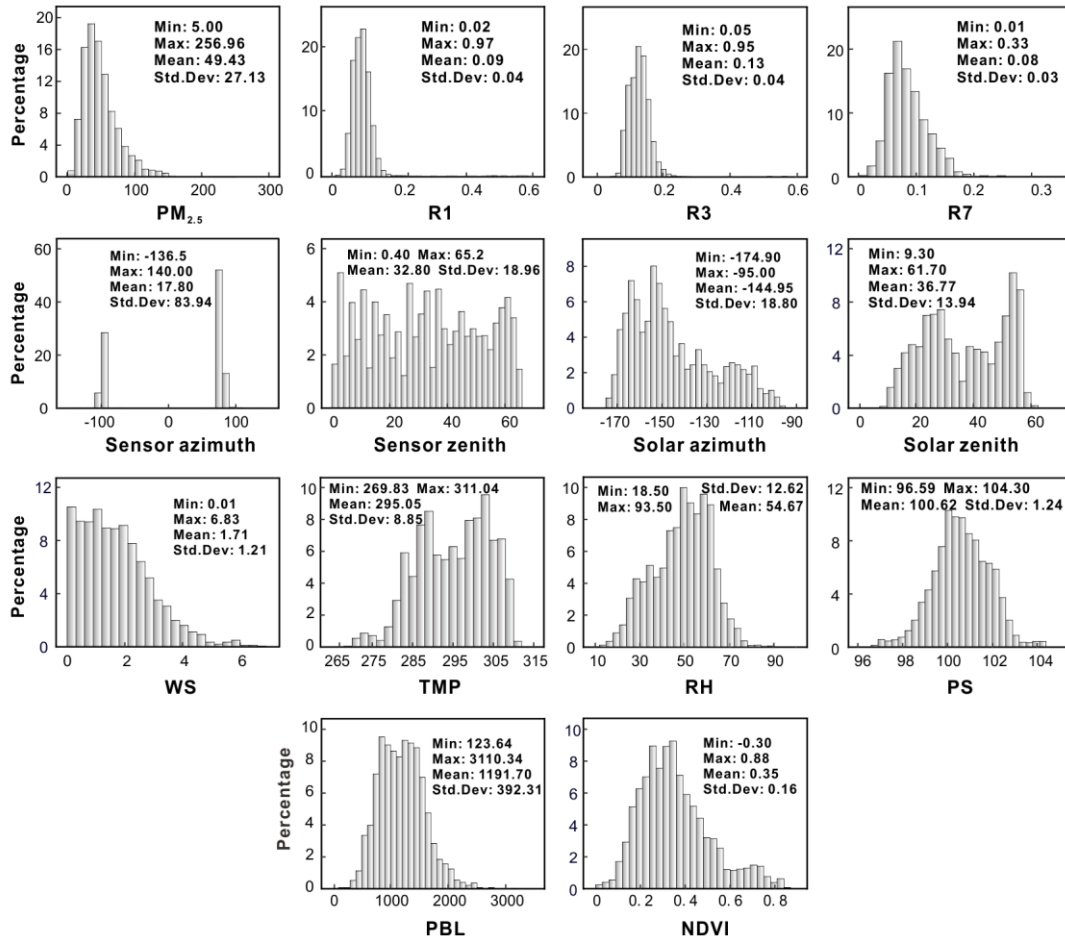


**Fig. 4.** Histograms and descriptive statistics of the Ref-PM modeling variables in the sample dataset.

Fig. 4 shows the histograms and descriptive statistics of the variables in the sample dataset. The  $PM_{2.5}$  concentrations range from  $5 \mu g / m^3$  to  $256.96 \mu g / m^3$ , with an average of  $49.43 \mu g / m^3$ . The R1, R3, and R7 are mostly distributed in 0~0.2, with mean values of 0.09, 0.13, and 0.08, respectively. It can be found that satellite TOA reflectance, temperature, relative humidity, surface pressure, height of planetary boundary layer, and NDVI have similar distribution patterns with  $PM_{2.5}$  concentration, while the observation angles and wind

speed have different distributions. The correlation coefficient between R1 (R3) and  $PM_{2.5}$  is 0.10 (0.12), indicating the nonlinear relationship between TOA reflectance and  $PM_{2.5}$ .

#### 4.2. Performance of the Ref-PM modeling

Fig. 5 shows the cross-validation performance of the Ref-PM modeling and the AOD-PM modeling, respectively. The sample size of the AOD-PM modeling dataset (N=1658) is much smaller than the Ref-PM modeling dataset (N=4181). The main reason is that the TOA reflectance data has a finer spatial resolution and larger coverage than the AOD product. For the Ref-PM modeling, an outstanding performance is achieved, with the sample-based (site-based) cross-validation  $R^2$  and RMSE values of 0.87 (0.79) and  $9.89$  ( $12.97$ )  $\mu g / m^3$ , respectively. Meanwhile, the sample-based (site-based) cross-validation  $R^2$  and RMSE of the AOD-PM modeling are 0.86 (0.72) and  $10.42$  ( $15.30$ )  $\mu g / m^3$ , respectively. We can observe that the sample-based cross-validation results of the Ref-PM modeling ( $R^2=0.87$ ) merely shows a slight advantage than that of the AOD-PM modeling ( $R^2=0.86$ ). Whilst the site-based cross-validation results of the AOD-PM modeling report a relatively larger decrease (from 0.79 to 0.72 for  $R^2$ ) compared with that of the Ref-PM modeling. It is worth noting that the site-based cross-validation approach, which uses a spatial hold-out validation strategy, can reflect the spatial predictive power more adequately (Li et al., 2017a). Hence, the results indicate that the Ref-PM modeling has a relatively superior spatial predictive power than the AOD-PM modeling.

On the other hand, the sample-based and site-based cross-validation slopes for the Ref-PM modeling are 0.87 and 0.82, respectively. This means that the proposed Ref-PM modeling tends to underestimate when the ground  $PM_{2.5}$  concentrations are greater than  $\sim 50 \mu g / m^3$ .

Meanwhile, the AOD-PM modeling reports a little higher extent of underestimation, with the sample-based and site-based cross-validation slopes of 0.82 and 0.79 respectively. The possible reason for this underestimation could be that we exploited point-based monitoring data and a spatially averaged modeling framework. The sampling distribution of monitoring stations in a grid may not give a great estimation of the spatially averaged concentration for that grid (Li et al., 2017a).

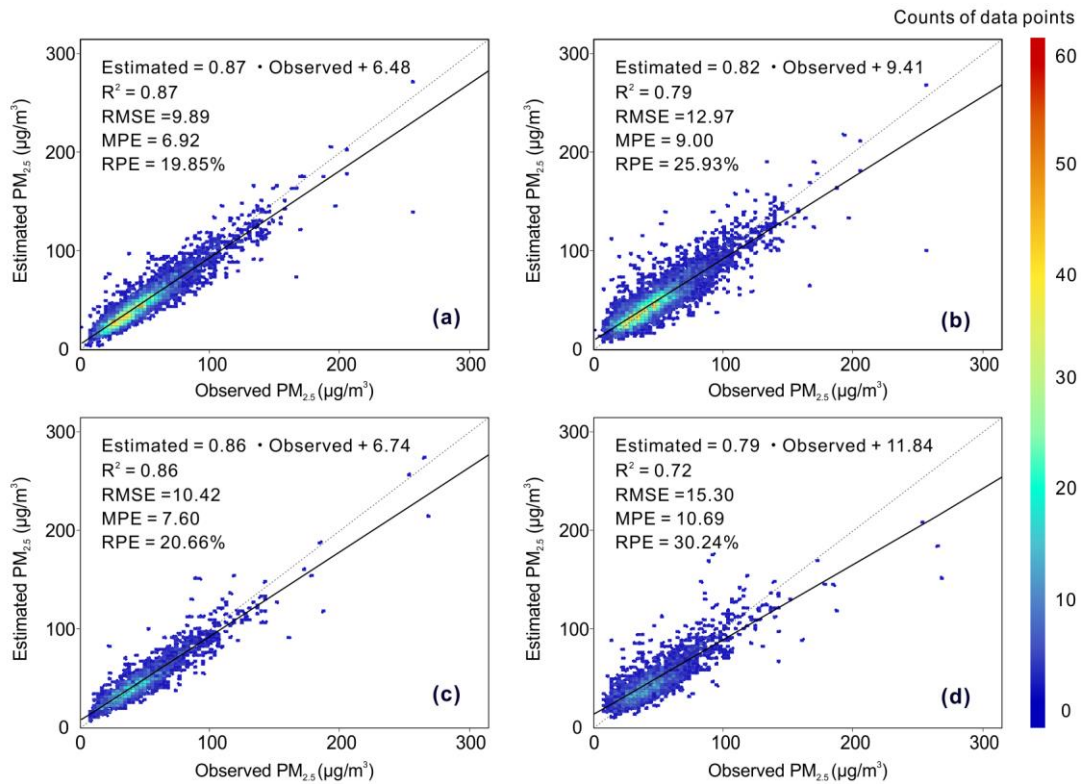


**Fig. 5.** Scatter plots of the Ref-PM modeling and the AOD-PM modeling cross-validation results: (a) and (b) are sample-based and site-based cross-validation results of the Ref-PM modeling (N=4181); (c) and (d) are sample-based and site-based cross-validation results of the AOD-PM modeling (N=1658).

Furthermore, the spatial site-based cross-validation performance of the Ref-PM modeling and the AOD-PM modeling was evaluated respectively. The  $R^2$  and RMSE values between the observed  $PM_{2.5}$  and estimated  $PM_{2.5}$  on each grid were calculated, which are shown in Fig. 6. Overall, the Ref-PM modeling has achieved a satisfactory performance, with 70% of grids reporting a high  $R^2$  value of greater than 0.80, and the low RMSE values ( $<15 \mu g / m^3$ ) are

found on 81% of grids. For the AOD-PM modeling, merely 59% of grids have  $R^2$  values of greater than 0.80, and the grids with RMSE values of less than  $15 \mu g / m^3$  account for 69%. These statistics indicate that the Ref-PM modeling shows some superiorities in the spatial prediction of  $PM_{2.5}$  than the AOD-PM modeling. Also, some spatial variations are observed in Fig. 6. For instance, compared with the results of the AOD-PM modeling, an obvious advantage is found in Wuhan for the Ref-PM modeling. On the contrary, the AOD-PM modeling achieves a slightly better result than the Ref-PM modeling in the regions of Xianning and Huanggang.

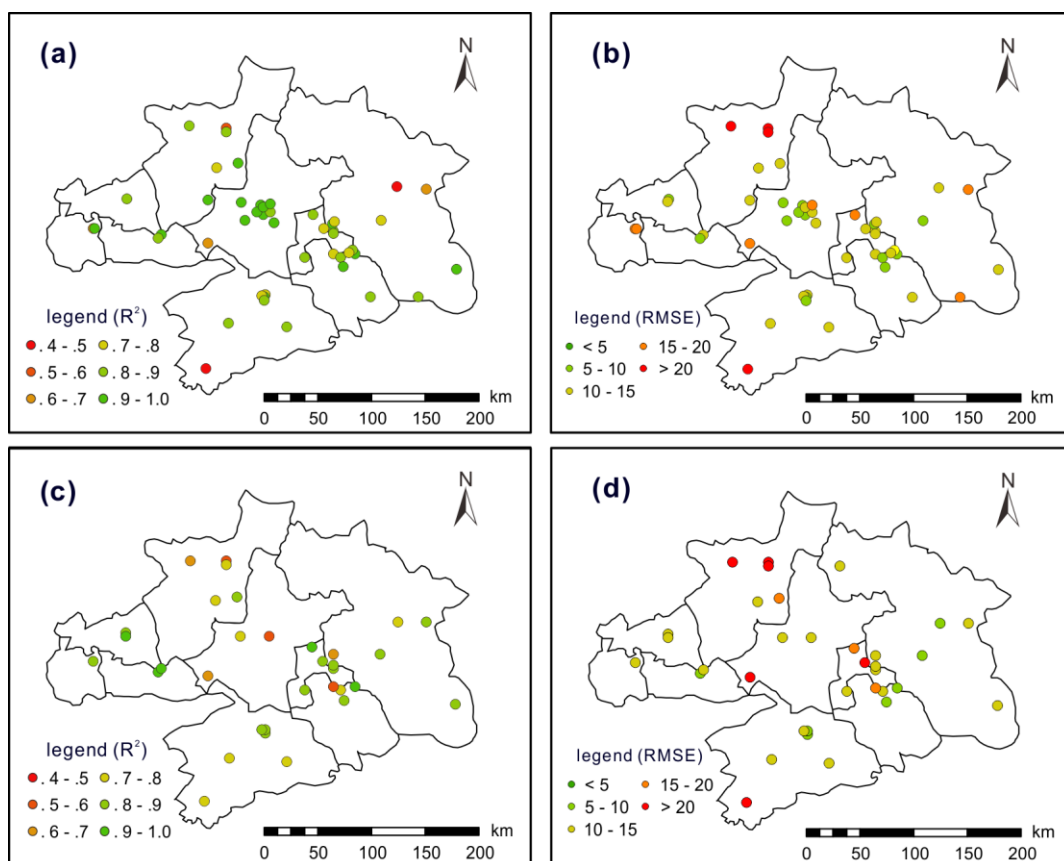


**Fig. 6.** Spatial performance of site-based cross-validation: (a) and (b) are  $R^2$  and RMSE for the Ref-PM modeling respectively; (c) and (d) are  $R^2$  and RMSE for the AOD-PM modeling respectively.

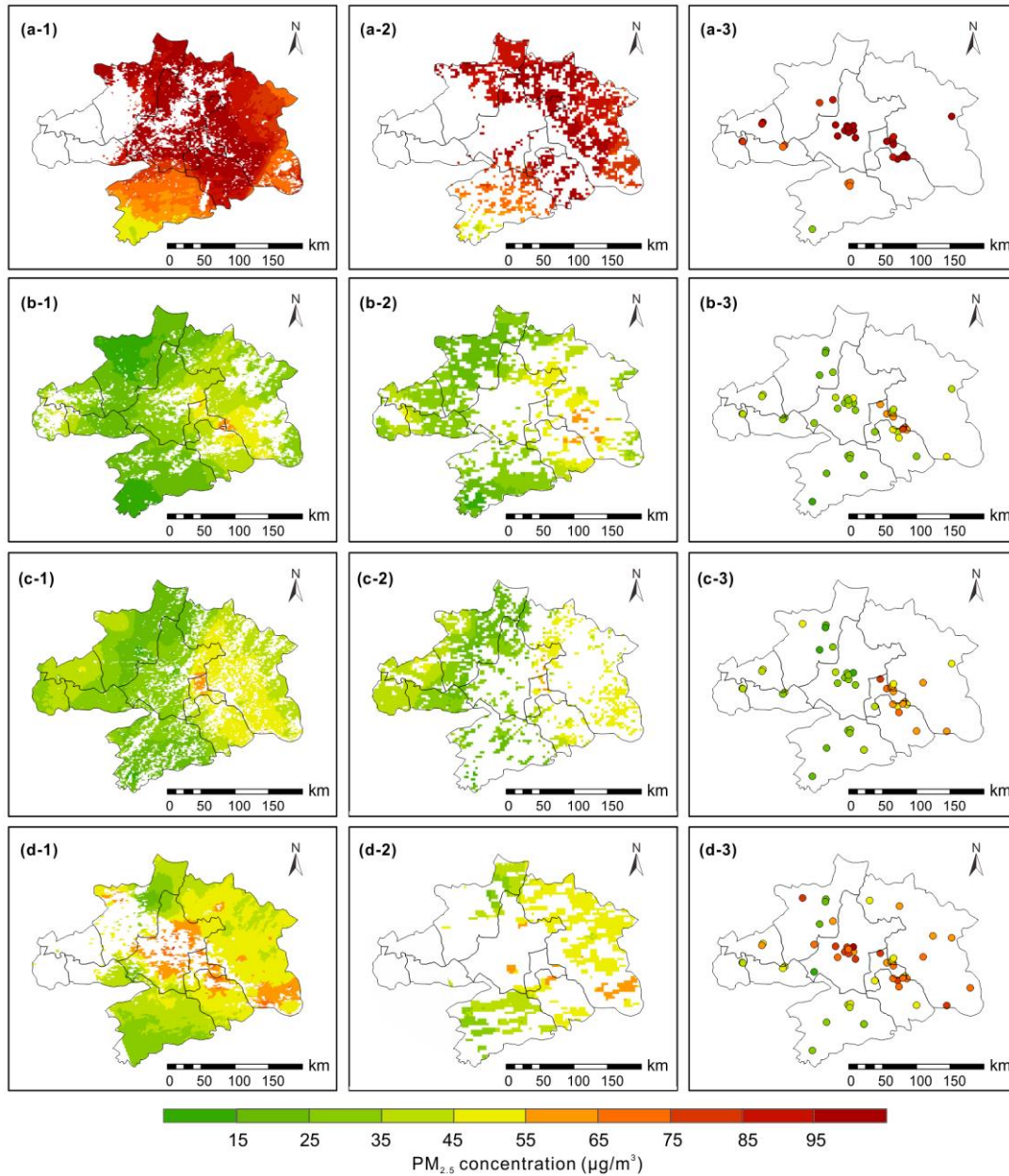


**Fig. 7.** Daily estimates of  $PM_{2.5}$  on some specific days (one day in each season), which have as much as valid data. From top to bottom: (a) 20160115, (b) 20160516, (c) 20160725, and (d) 20161127. Left column: TOA reflectance-based estimation of  $PM_{2.5}$ . Middle column: AOD-based estimation of  $PM_{2.5}$ . Right column: ground station measurements. The white regions indicate missing data.

#### 4.3. Discussion

The retrieval of AOD often meets a challenge, which is the bright surfaces ( $R7 > 0.15$ ) (Li et al., 2005). Thus, the AOD-based estimation of  $PM_{2.5}$  may be missing on the bright surface regions. In this paper, the TOA reflectance on bright surface have been included to estimate

ground-level PM<sub>2.5</sub>. As illustrated in Fig. 7, the reflectance-derived PM<sub>2.5</sub> have larger spatial coverage than the AOD-derived PM<sub>2.5</sub>, which can largely be attributed to the estimates on bright surfaces. We evaluate the performance of the Ref-PM modeling on the bright surfaces. The results show that the sample-based cross-validated R<sup>2</sup> value is 0.80 on the bright surface regions, and 0.87 on the dark target regions. We can see that the accuracy of PM<sub>2.5</sub> estimation on bright surfaces is acceptable. Also, the reflectance-derived PM<sub>2.5</sub> have a smooth tendency in space (Fig. 7). The results indicate that the Ref-PM modeling has the potential to provide larger coverage of valid PM<sub>2.5</sub> estimates than the AOD-PM modeling. As is further observed in Fig. 7, the reflectance-derived PM<sub>2.5</sub> have a finer resolution than the AOD-derived PM<sub>2.5</sub>, so that more details of PM<sub>2.5</sub> distributions are able to be investigated. These findings reveal that the reflectance-derived PM<sub>2.5</sub> have a finer resolution and more valid estimates on bright surfaces than the AOD-derived PM<sub>2.5</sub>.

This study provides an effective solution for the estimation of ground-level PM<sub>2.5</sub> from satellite TOA reflectance rather than AOD products. However, the satellite-derived AOD is still one of the import atmospheric parameters. For example, the satellite-derived AOD itself is an indicator of atmospheric pollution, and plays an important role in the researches on aerosol-cloud interaction, climate changes, etc. This paper merely says that as for the estimation of ground-level PM<sub>2.5</sub>, it appears possible to avoid the retrieval of satellite AOD. The proposed solution can also be extended to the monitoring of other environmental features, especially when no proper satellite parameters like AOD are found. Therefore, this study has no intention to belittle AOD retrieval or the AOD-PM modeling, but emphasizes on developing a new solution for the satellite-based estimation of PM<sub>2.5</sub>.

## 5. Conclusions and future work

In this paper, the Ref-PM modeling is developed to avoid the intermediate process of AOD retrieval, and to estimate ground-level  $PM_{2.5}$  directly from satellite TOA reflectance without a physical model. More importantly, this Ref-PM modeling has the potential to be extended to the satellite-based monitoring of other environmental features. Using the Wuhan Urban Agglomeration (WUA) as an example, the results show that compared with the AOD-PM modeling, the Ref-PM modeling achieves a competitive performance, with sample-based cross-validation  $R^2$  and RMSE values of 0.87 and  $9.89 \mu g / m^3$  respectively. Also, the daily distributions of  $PM_{2.5}$  in WUA are mapped, and the reflectance-derived  $PM_{2.5}$  have a finer resolution and larger spatial coverage than the AOD-derived  $PM_{2.5}$ . All these results can say that the proposed Ref-PM modeling has the capacity to estimate ground-level  $PM_{2.5}$  concentration directly from satellite TOA reflectance. This work updates the traditional cognition of remote sensing  $PM_{2.5}$  estimation and can provide useful information for the pollution monitoring and control.

The future studies will focus on two aspects. Firstly, the Ref-PM modeling has achieved some reasonable results for the estimation of  $PM_{2.5}$  directly from TOA reflectance. However, we only selected R1, R3, R7, and observation angles for the model establishment. The selection is inspired by dark target algorithm (Kaufman et al., 1997). Will the incorporation of surface reflectance data (e.g., MOD09) boost the accuracy of  $PM_{2.5}$  estimation? Whether or not more/other satellite parameters can better explain  $PM_{2.5}$  concentration still has room for researching. Secondly, the proposed Ref-PM modeling is validated in a small region of WUA in this study. It may bring out new challenges and problems in larger geographical regions.

The application and validation of the Ref-PM modeling in large geographical regions will be conducted in the future studies.

### **Acknowledgments**

This work was funded by the National Key R&D Program of China (2016YFC0200900) and the National Natural Science Foundation of China (41422108). We are grateful to the China National Environmental Monitoring Center (CNEMC), the Hubei Provincial Environmental Monitoring Center Station (HPEMCS), the Goddard Space Flight Center Distributed Active Archive Center (GSFC DAAC), the US National Aeronautics and Space Administration (NASA) Data Center for providing the foundational data.

## Reference

- Ackerman, S.A., Strabala, K.I., Menzel, W.P., Frey, R.A., Moeller, C.C., & Gumley, L.E. (1998). Discriminating clear sky from clouds with MODIS. *Journal of Geophysical Research: Atmospheres*, *103*, 32141-32157
- Engel-Cox, J., Kim Oanh, N.T., van Donkelaar, A., Martin, R.V., & Zell, E. (2013). Toward the next generation of air quality monitoring: Particulate Matter. *Atmospheric Environment*, *80*, 584-590
- Fang, X., Zou, B., Liu, X., Sternberg, T., & Zhai, L. (2016). Satellite-based ground PM<sub>2.5</sub> estimation using timely structure adaptive modeling. *Remote Sensing of Environment*, *186*, 152-163
- Gupta, P., & Christopher, S.A. (2009a). Particulate matter air quality assessment using integrated surface, satellite, and meteorological products: 2. A neural network approach. *Journal of Geophysical Research: Atmospheres*, *114*, D20205
- Gupta, P., & Christopher, S.A. (2009b). Particulate matter air quality assessment using integrated surface, satellite, and meteorological products: Multiple regression approach. *Journal of Geophysical Research: Atmospheres*, *114*, D14205
- Habre, R., Moshier, E., Castro, W., Nath, A., Grunin, A., Rohr, A., Godbold, J., Schachter, N., Kattan, M., Coull, B., (2014). The effects of PM<sub>2.5</sub> and its components from indoor and outdoor sources on cough and wheeze symptoms in asthmatic children. *J Expos Sci Environ Epidemiol*, *24*, 380-387
- Hinton, G.E., Osindero, S., & Teh, Y.-W. (2006). A fast learning algorithm for deep belief nets. *Neural computation*, *18*, 1527-1554
- Hoff, R.M., & Christopher, S.A. (2009). Remote Sensing of Particulate Pollution from Space: Have We Reached the Promised Land? *Journal of the Air & Waste Management Association*, *59*, 645-675
- Hsu, N.C., Tsay, S.-C., King, M.D., & Herman, J.R. (2004). Aerosol properties over bright-reflecting source regions. *IEEE Transactions on Geoscience and Remote Sensing*, *42*, 557-569
- Hu, X., Waller, L.A., Al-Hamdan, M.Z., Crosson, W.L., Estes Jr, M.G., Estes, S.M., Quattrochi, D.A., Sarnat, J.A., & Liu, Y. (2013). Estimating ground-level PM<sub>2.5</sub> concentrations in the southeastern U.S. using geographically weighted regression. *Environmental Research*, *121*, 1-10
- Kaufman, Y.J., Tanré D., Remer, L.A., Vermote, E.F., Chu, A., & Holben, B.N. (1997). Operational remote sensing of tropospheric aerosol over land from EOS moderate resolution imaging spectroradiometer. *Journal of Geophysical Research: Atmospheres*, *102*, 17051-17067
- Lee, H., Liu, Y., Coull, B., Schwartz, J., & Koutrakis, P. (2011). A novel calibration approach of MODIS AOD data to predict PM<sub>2.5</sub> concentrations. *Atmospheric Chemistry and Physics*, *11*, 7991-8002
- Levy, R.C., Remer, L.A., Mattoo, S., Vermote, E.F., & Kaufman, Y.J. (2007). Second-generation operational

algorithm: Retrieval of aerosol properties over land from inversion of Moderate Resolution Imaging Spectroradiometer spectral reflectance. *Journal of Geophysical Research: Atmospheres*, 112, n/a-n/a

Li, C., Lau, A.K.H., Mao, J., & Chu, D.A. (2005). Retrieval, validation, and application of the 1-km aerosol optical depth from MODIS measurements over Hong Kong. *IEEE Transactions on Geoscience and Remote Sensing*, 43, 2650-2658

Li, T., Shen, H., Yuan, Q., Zhang, X., & Zhang, L. (2017a). Estimating Ground-Level PM<sub>2.5</sub> by Fusing Satellite and Station Observations: A Geo-Intelligent Deep Learning Approach. *Geophysical Research Letters*, 44, 11,985-911,993

Li, T., Shen, H., Zeng, C., Yuan, Q., & Zhang, L. (2017b). Point-surface fusion of station measurements and satellite observations for mapping PM<sub>2.5</sub> distribution in China: Methods and assessment. *Atmospheric Environment*, 152, 477-489

Li, Z., Zhang, Y., Shao, J., Li, B., Hong, J., Liu, D., Li, D., Wei, P., Li, W., Li, L., (2016). Remote sensing of atmospheric particulate mass of dry PM<sub>2.5</sub> near the ground: Method validation using ground-based measurements. *Remote Sensing of Environment*, 173, 59-68

Lim, S.S., Vos, T., Flaxman, A.D., Danaei, G., Shibuya, K., Adair-Rohani, H., AlMazroa, M.A., Amann, M., Anderson, H.R., Andrews, K.G., (2012). A comparative risk assessment of burden of disease and injury attributable to 67 risk factors and risk factor clusters in 21 regions, 1990–2010: a systematic analysis for the Global Burden of Disease Study 2010. *The Lancet*, 380, 2224-2260

Lucchesi, R. (2013). File Specification for GEOS-5 FP. In. GMAO Office Note No. 4 (Version 1.0)

Ma, Z., Hu, X., Huang, L., Bi, J., & Liu, Y. (2014). Estimating Ground-Level PM<sub>2.5</sub> in China Using Satellite Remote Sensing. *Environmental Science & Technology*, 48, 7436-7444

Madrigano, J., Kloog, I., Goldberg, R., Coull, B.A., Mittleman, M.A., & Schwartz, J. (2013). Long-term Exposure to PM<sub>2.5</sub> and Incidence of Acute Myocardial Infarction. *Environmental Health Perspectives*, 121, 192-196

Munchak, L.A., Levy, R.C., Mattoo, S., Remer, L.A., Holben, B.N., Schafer, J.S., Hostetler, C.A., & Ferrare, R.A. (2013). MODIS 3 km aerosol product: applications over land in an urban/suburban region. *Atmos. Meas. Tech.*, 6, 1747-1759

Ong, B.T., Sugiura, K., & Zettsu, K. (2015). Dynamically pre-trained deep recurrent neural networks using environmental monitoring data for predicting PM<sub>2.5</sub>. *Neural Computing and Applications*, 1-14

Paciorek, C.J., Liu, Y., Moreno-Macias, H., & Kondragunta, S. (2008). Spatiotemporal Associations between GOES Aerosol Optical Depth Retrievals and Ground-Level PM<sub>2.5</sub>. *Environmental Science & Technology*, 42, 5800-5806

Radosavljevic, V., Vucetic, S., & Obradovic, Z. (2007). Aerosol optical depth retrieval by neural networks

ensemble with adaptive cost function. In, *the 10th International Conference on Engineering Applications of Neural Networks* (pp. 266-275)

Ristovski, K., Vucetic, S., & Obradovic, Z. (2012). Uncertainty Analysis of Neural-Network-Based Aerosol Retrieval. *IEEE Transactions on Geoscience and Remote Sensing*, *50*, 409-414

Rodriguez, J.D., Perez, A., & Lozano, J.A. (2010). Sensitivity Analysis of k-Fold Cross Validation in Prediction Error Estimation. *IEEE Transactions on Pattern Analysis and Machine Intelligence*, *32*, 569-575

Rumelhart, D.E., Hinton, G.E., & Williams, R.J. (1986). Learning representations by back-propagating errors. *Nature*, *323*, 533-536

Sorek-Hamer, M., Kloog, I., Koutrakis, P., Strawa, A.W., Chatfield, R., Cohen, A., Ridgway, W.L., & Broday, D.M. (2015). Assessment of PM<sub>2.5</sub> concentrations over bright surfaces using MODIS satellite observations. *Remote Sensing of Environment*, *163*, 180-185

van Donkelaar, A., Martin, R.V., Brauer, M., Hsu, N.C., Kahn, R.A., Levy, R.C., Lyapustin, A., Sayer, A.M., & Winker, D.M. (2016). Global Estimates of Fine Particulate Matter using a Combined Geophysical-Statistical Method with Information from Satellites, Models, and Monitors. *Environmental Science & Technology*, *50*, 3762-3772

Wang, L., Gong, W., Li, J., Ma, Y., & Hu, B. (2014). Empirical studies of cloud effects on ultraviolet radiation in Central China. *International Journal of Climatology*, *34*, 2218-2228

Wang, L., Gong, W., Xia, X., Zhu, J., Li, J., & Zhu, Z. (2015). Long-term observations of aerosol optical properties at Wuhan, an urban site in Central China. *Atmospheric Environment*, *101*, 94-102

Wu, J., Yao, F., Li, W., & Si, M. (2016). VIIRS-based remote sensing estimation of ground-level PM<sub>2.5</sub> concentrations in Beijing–Tianjin–Hebei: A spatiotemporal statistical model. *Remote Sensing of Environment*, *184*, 316-328

Xie, Y., Wang, Y., Zhang, K., Dong, W., Lv, B., & Bai, Y. (2015). Daily estimation of ground-level PM<sub>2.5</sub> concentrations over Beijing using 3 km resolution MODIS AOD. *Environmental Science & Technology*, *49*, 12280-12288

Yang, Q., Yuan, Q., Li, T., Shen, H., & Zhang, L. (2017). The Relationships between PM<sub>2.5</sub> and Meteorological Factors in China: Seasonal and Regional Variations. *International Journal of Environmental Research and Public Health*, *14*

You, W., Zang, Z., Pan, X., Zhang, L., & Chen, D. (2015). Estimating PM<sub>2.5</sub> in Xi'an, China using aerosol optical depth: A comparison between the MODIS and MISR retrieval models. *Science of The Total Environment*, *505*, 1156-1165